35th Annual International Conference of the IEEE EMBS
Osaka, Japan, 3 - 7 July, 2013

Analysis and Modeling of Noise in Biomedical Systems

Mina Ranjbaran, Kian Jalaleddini, Diego Guarin Lopez, Robert E. Kearney and Henrietta L. Galiana

Abstract— **Noise characteristics play an important role in evaluating tools developed to study biomedical systems. Despite usual assumptions, noise in biomedical systems is often non-white or non-Gaussian. In this paper, we present a method to analyze the noise component of a biomedical system. We demonstrate the effectiveness of the method in the analysis of noise in voluntary ankle torque measured by a torque transducer and eye movements measured by electro-oculography (EOG).**

I. Introduction

Noise is an unwanted random series that corrupts the signals of interest [1]. Biomedical signal measurements are often contaminated with considerable noise from different sources, such as: thermal noise, interfering signals from the body, environment or electrode movements [2].

Analysis of noise is an important problem and is well studied in medical imaging [1], [3]. Noise characteristics also play a leading role in selecting identification tools for biomedical systems where the goal is to estimate a model that represents the input-output relation. Often, in the model formulation, the noise signal is assumed to be independently and identically distributed i.i.d. (white) and/or Gaussian [4]–[8] when algorithms are chosen. Yet, this assumption may not be valid in reality. As a result, the efficiency and robustness of the applied methods could be evaluated incorrectly and cause biased identifications. Moreover, a realistic noise model can be used in creating virtual data sets for the validation of selected methods for system identification, data classification, etc.

Noise analysis can also provide useful physiological information. For example, in the identification of joint stiffness using small signal models, voluntary torques appear as a noise background. The characteristics of this noise component can reveal the bandwidth of the torque or the frequency of a tremor if present [9], [10].

In closed-loop models with output feedback, the additive output noise is combined with the input reference signal. This results in a challenging system identification which requires special treatments to account for the input noise. Consequently, knowledge about the noise characteristics is important in such problems [11], [12].

In this work, we present a method to analyze a biomedical noise signal. Our hypothesis is that this signal is not necessarily white and Gaussian and might have its own dynamics that can differ from that of the system. We model the noise signal as the output of a stochastic system whose input is a white random sequence. Thus, we fit an *autoregressive model* (AR) model. This model is equivalent to an *impulse response function* (IRF). Consequently, the method is non-parametric and does not require much *a priori* information about the model order. We then use this method to analyze two case studies during near constant self-generated responses (no control stimulus): *(i)* torque measurements from the ankle joint while maintaining the joint torque and *(ii)* EOG signals recorded in the dark while attempting to fix gaze in space.

The rest of the paper is organized as follows: Section II formulates the model and describes the methodology. Section III provides results for the two case studies. Section IV concludes with a summary and potential applications.

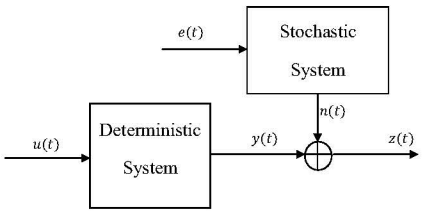

Fig. 1. Deterministic and stochastic components of a biomedical system.

II. Methods

Fig. 1 shows a schematic of a biomedical system. The input $u(t)$ enters the deterministic plant. A *white* signal $e(t)$ enters the stochastic plant which generates the additive noise signal $n(t)$. Thus, the measured output is: $z(t) = n(t)+y(t)$.

The objective is to analyze the stochastic system that generates the noise signal. Therefore, the first step is to remove the deterministic system by recording the output signal in the absence of any forced input component. The observed noise sequence (output) is then a combination of three main components: *(i)* noise as a result of electronics, *(ii)* output of the biomedical system with only an internal set-point, and *(iii)* a non-stationary component as a result of the time-varying nature of the biomedical system.

Noise generated by the electronics generally contains a white random sequence introduced by thermal/shot noise, plus 60Hz with harmonics induced by the power line and its nonlinear elements. This component can be observed by recording from the electronics in the absence of the biomedical system. For example, Fig. 2 shows the characteristics of the recorded signal from a torque transducer intended for the ankle joint torque measurements, but in the absence of a subject. The sampling frequency was 1KHz for 120s of data. The frequency structure shows the white dynamics of the noise (flat spectrum), carrying spikes of 60Hz noise with

This work is supported by CIHR and NSERC.

Authors are with the Department of Biomedical Engineering, McGill University, Montreal, Canada, H3A 2B4.
Email: mina.ranjbaranhesarmaskan@mail.mcgill.ca

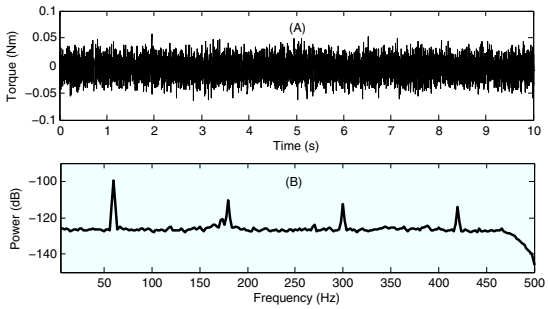

Fig. 2. Noise due to electronics in recording torque with no subject: (A) 10s realization of the noise; (B) frequency spectrum.

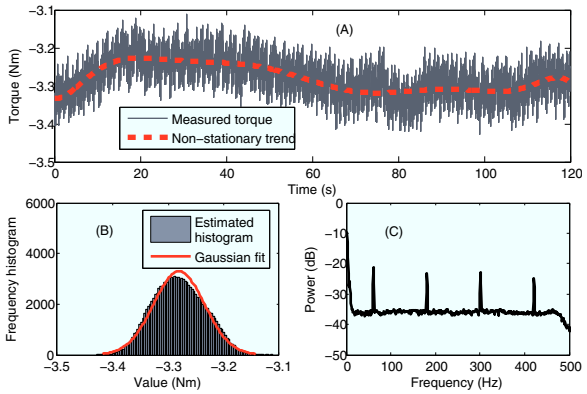

Fig. 3. Recorded torque from ankle joint in presence of a subject; (A) Time realization; (B) Amplitude frequency histogram; (C) Frequency spectrum.

its harmonics, as well as the dynamics of the anti-aliasing filter (low-pass filter at 480HZ) causing low power at high frequencies.

We selected an AR structure to describe the stochastic system dynamics. The AR model is straightforward to implement, does not require much *a priori* information and the model formulation is linear in its parameters. However, there are some challenges.

First, biomedical system dynamics usually change very slowly in time (e.g. fatigue, alertness). Hence, the non-stationary component of the noise will also have low-pass dynamics. To capture this, an AR model would require a large memory, i.e. a large number of parameters in Equ. 2 below, equal to data length. To avoid this problem, we can either high-pass filter the data at a low break frequency or remove a polynomial trend from the data record.

Second, there is the issue of 60Hz noise and its harmonics (Fig. 2). Modeling this component within the AR model also requires an IRF with many lags. Instead, we remove these periodic components before fitting the AR model, using notch filters at those frequencies.

For instance, a non-stationary behavior is observed in a torque record from a subject's ankle joint (Fig. 3.A) while maintaining constant torque level (120s with 1KHz sampling rate). The estimated amplitude histogram (Fig. 3.B) does not show a perfect Gaussian distribution. The frequency spectrum (Fig. 3.C) shows a non-white signal that has relatively large power at low-frequencies besides the 60Hz noise harmonics and anti-aliasing dynamics of Fig. 2.

Once the periodic and non-stationary components are removed, we fit an AR model to the remaining noise, $r(t)$, assuming a white input, $e(t)$, to the stochastic model. The AR structure with n_a IRF lags has the following formulation:

$$\frac{r(z)}{e(z)} = \frac{1}{1 + a_1 z^{-1} + \cdots + a_{n_a} z^{-n_a}} \tag{1}$$

where z is the Z transform variable and a_i for $i = 1, \cdots, n_a$ are the unknown model coefficients to be estimated. Let N be the number of recorded data samples, i.e. $t \in \{1, \cdots, N\}$. We expand Equ. 1 to the following data equation:

$$\begin{bmatrix} r(1) \\ r(2) \\ \vdots \\ r(N) \end{bmatrix} = \underbrace{\begin{bmatrix} 0 & \cdots & 0 \\ -r(1) & \cdots & 0 \\ \vdots & \ddots & \vdots \\ -r(N-1) & \cdots & -r(N-n_a) \end{bmatrix}}_{\Psi} \begin{bmatrix} a_1 \\ a_2 \\ \vdots \\ a_{n_a} \end{bmatrix} + \begin{bmatrix} e(1) \\ e(2) \\ \vdots \\ e(N) \end{bmatrix} \tag{2}$$

We solve Equ. 2 using least-squares approach:

$$\begin{bmatrix} \hat{a}_1 & \hat{a}_2 & \cdots & \hat{a}_{n_a} \end{bmatrix}^T = \Psi^\dagger \begin{bmatrix} r(1) & r(2) & \cdots & r(N) \end{bmatrix}^T \tag{3}$$

where $\dagger$ is the pseudo inverse operation and $\hat{a}_i$ for $i = 1, \cdots, n_a$ are the estimated coefficients. $e(t)$ needs to be examined for whiteness since this was the AR model assumption. Note that here, $e(t)$ is also the fit residual. A sufficient number of lags, n_a, is needed to obtain a white $e(t)$.

III. Results

In this section, we verified the method by studying two bio-signals. The first was the ankle joint torque recorded using a torque transducer. The second was eye movements recorded using EOG sensors. In these experiments the recruited subjects gave informed consent to the experimental procedures, which had been reviewed and approved by McGill University Institutional Review Board.

A. Voluntary Torque Analysis

The subject laid supine while the left foot was attached to a position-servo hydraulic actuator. The angle between foot and shank was set to 90°. The actuator was much stiffer than the subject ankle, i.e. subjects could not move the actuator. We recorded the ankle torque from a torque transducer placed in series between the ankle and actuator for 120s with a sampling rate of 1KHz. The experimental conditions were similar to those explained in [13]. But here, subjects were asked to maintain a constant torque. Fig. 3.A shows a realization of the recorded torque. We divided data into two segments of 60s and analyzed each with the presented

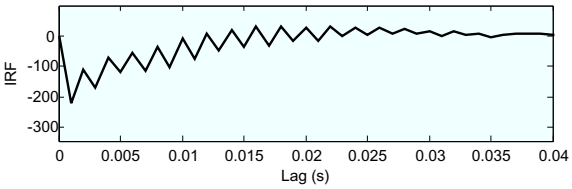

Fig. 4. IRF of the estimated AR model for torque recordings.

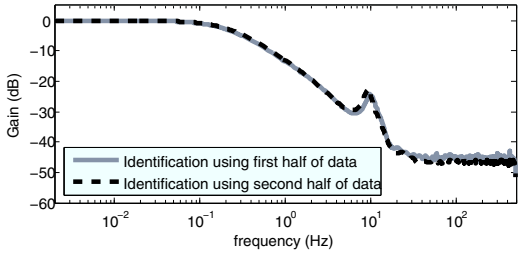

Fig. 5. Magnitude of the transfer function of the identified torque noise AR model.

method. The non-stationary component was removed by high-pass filtering (break frequency of 0.01Hz) and 60Hz harmonics were notch-filtered. The number of lags n_a for the AR model was set to 145 in order to obtain white $e(t)$.

Fig. 4 shows the estimated AR model (only the significant first 40 lags are shown). The IRF shows gradual increase in time and an oscillation. Thus, it demonstrates that the stochastic system had a low-pass behavior plus an oscillatory component. Fig. 5 shows the magnitude plot of the identified AR models for both data segments. Both models had overlapping dynamics, so the noise characteristics were consistent in both data segments. Thus, the identified voluntary torque model is a low-pass filter with a resonance at 9Hz, in the range of reported physiological tremor [10].

Fig. 6 shows the autocorrelation coefficient and amplitude structure of $e(t)$. The autocorrelation coefficient had a spike at zero. This shows that $e(t)$ was white and the AR model assumption was valid. The amplitude structure of $e(t)$ was also well described with a Gaussian distribution.

B. EOG Analysis

In this experiment, EOG surface electrodes were placed on the skin on the temporal side of each eye and on the

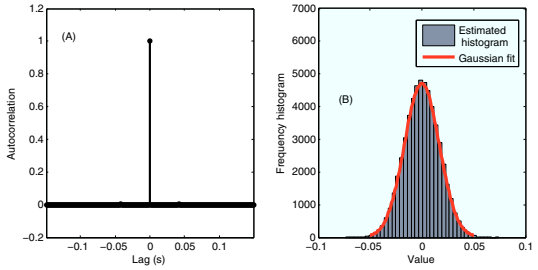

Fig. 6. Analysis of the fit residual, $e(t)$: (A) Autocorrelation coefficient, (B) Amplitude frequency histogram.

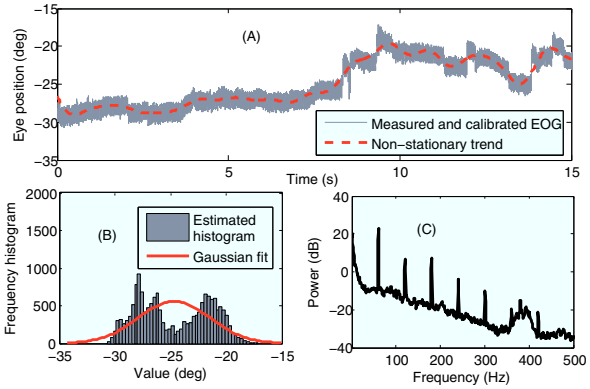

Fig. 7. Recorded EOG in the dark (A) Time realization; B) Amplitude frequency histogram; (C) Frequency spectrum.

forehead (ground). The subject was seated in the dark for 20 minutes for stabilization of ocular and electrode potentials in the dark. The subject was then secured on a chair with the head restrained to a head rest and asked to fixate on a flashed target appearing for 5s and extinguished for 15s. A new flashed target appeared at a different location every 20s repeating the pattern. Eye movements were recorded in darkness with stationary head at a sampling rate of 1KHz. The experimental conditions and calibration procedure are described in [14], where the study explored gaze holding in the dark with no visual inputs. Fig. 7.A shows a realization of such recorded EOG for one 15s fixation interval with the non-stationary trend marked in red. Such trends in the dark are caused by gaze holding decay (electrode drift was removed in the calibration procedure). The histogram (Fig. 7.B) is clearly different from a Gaussian model due to this non-stationarity and 60Hz harmonics from electrical noise in EOG recordings. The frequency spectrum (Fig. 7.C) also shows low-pass behavior and confirms 60Hz harmonic components.

We removed the non-stationary trend by high-pass filtering at 0.5Hz and notch filtering the 60Hz harmonics. The number of lags n_a for AR model was set to 250 to obtain white fit residuals, $e(t)$.

Fig. 8 shows the estimated AR model for the remaining noise (only the significant first 40 lags are shown). It has a low-pass behavior plus an oscillatory component. Fig. 9 shows the magnitude plot of the identified AR models for two data segments recorded during the same experiment but at *different* fixation points [14]. Estimated noise models from both data segments have similar dynamics which implies that the fixation point did not modulate the noise properties. Thus, the identified EOG noise model was a low-pass filter with a resonance at 2Hz, in the range of reported micro-saccade frequency during fixation [15].

Fig. 10 provides the autocorrelation coefficient and amplitude structure of $e(t)$. Whiteness of $e(t)$ from its autocorrelation confirms that the AR model order was correct.

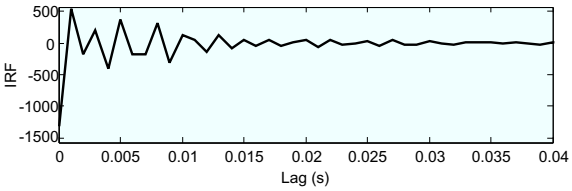

Fig. 8. IRF of the estimated AR model for EOG recordings.

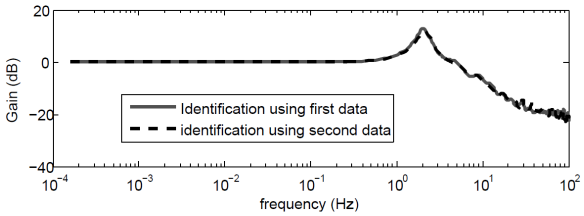

Fig. 9. Magnitude of the transfer function of the identified EOG noise AR model.

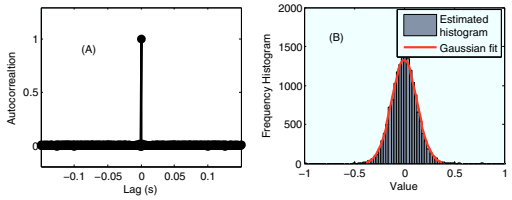

Fig. 10. Analysis of the fit residual, $e(t)$: (A) Autocorrelation coefficient, (B) Amplitude frequency histogram.

IV. Conclusion

Assuming white/Gaussian noise is not always valid in biomedical systems. In this paper, a method is presented to analyze noise in biomedical systems. It includes recording from subjects in the absence of controlled inputs. We propose removing low-frequency non-stationary components and 60Hz noise harmonics to study imbedded stochastic properties - that is, high-pass filtering at appropriate frequencies to remove contributions from the associated deterministic system, and notch filtering electronic noise components. The dynamics of the remaining noise is then represented by an AR model. This non-parametric method can be adopted in different applications with only one easily adjustable free parameter, i.e. the number of lags in the IRF model.

We applied our method to analyze noise in voluntary torque measurements and EOG recordings, when the task was simply to maintain the set-point. Both types of recordings were shown to contain noise signals that were not necessarily Gaussian nor white. Modeling the noise revealed the frequency of physiological tremor in torque measurements and micro-saccades in EOG recordings. Similar subconscious components can be found in all biomedical recordings and must be taken into account in order to obtain unbiased models for the deterministic system reacting to forced stimuli. Hence, noise properties cannot be assumed *a priori*. They must be examined in each case in order to select correct algorithms for model identification.

Two other applications can be envisioned. First, by replicating noise components in model simulations (restoring stochastic model and even electrical noise harmonics), one can create realistic virtual data on which to validate proposed identification algorithms. The advantage would be to test convergence and robustness in the presence of noise similar to experimental conditions rather than relying on white/Gaussian assumptions. Here, both temporal and amplitude characteristics of expected noise could be duplicated. Second, biological noise characteristics in general can vary with context (e.g. limb position, load, stimulus conditions), or even with/without the presence of a controlled input. Thus, noise needs to be examined for each protocol and laboratory.

Finally, unmasking noise components can lead to more accurate deterministic models. For example, deciding whether components like tremor should be included in the characteristics of the deterministic system, or left to the stochastic component. Or in a similar vein, whether the low-frequency trends are really noise, or are consistent with the dynamics or poles of the deterministic system (e.g. decay profiles).

References

[1] B. Friedlander and A. Weiss, "Direction finding using noise covariance modeling," *Signal Processing, IEEE Transactions on*, vol. 43, no. 7, pp. 1557–1567, 1995.

[2] J. Webster, *Medical Instrumentation: Application And Design, 3Rd Ed*. Wiley India Pvt. Limited, 2009.

[3] O. Michailovich and A. Tannenbaum, "Despeckling of medical ultrasound images," *IEEE Trans. Ultrason., Ferroelect., Freq. Contr*, vol. 53, pp. 64–78, 2006.

[4] S. Kukreja, H. Galiana, and R. Kearney, "Narmax representation and identification of ankle dynamics," *Biomedical Engineering, IEEE Transactions on*, vol. 50, pp. 70 –81, jan. 2003.

[5] S. Kukreja, R. Kearney, and H. Galiana, "A least-squares parameter estimation algorithm for switched hammerstein systems with applications to the vor," *Biomedical Engineering, IEEE Transactions on*, vol. 52, pp. 431 –444, march 2005.

[6] L. Ljung, *System Identification: Theory for the User*. Pearson Education, 1998.

[7] A. Chiuso, "On the relation between cca and predictor-based subspace identification," *Automatic Control, IEEE Transactions on*, vol. 52, pp. 1795 –1812, oct. 2007.

[8] M. Verhaegen and V. Verdult, *Filtering and System Identification: A Least Squares Approach*. New York, NY, USA: Cambridge University Press, 1st ed., 2007.

[9] L. Galiana, J. Fung, and R. Kearney, "Identification of intrinsic and reflex ankle stiffness components in stroke patients," *Experimental Brain Research*, vol. 165, pp. 422–434, 2005.

[10] R. J. Elble, "Physiologic and essential tremor," *Neurology*, vol. 36, no. 2, p. 225, 1986.

[11] Y. Zhao, D. Ludvig, and R. Kearney, "Closed-loop system identification of ankle dynamics using a subspace method with reference input as instrumental variable," in *American Control Conference, 2008*, pp. 619 –624, june 2008.

[12] M. Verhaegen, "Application of a subspace model identification technique to identify lti systems operating in closed-loop," *Automatica*, vol. 29, no. 4, pp. 1027 – 1040, 1993.

[13] D. Ludvig, Y. Zhao, and R. E. Kearney, "Control of an unstable load using visual feedback," in *Engineering in Medicine and Biology Society, 2008. EMBS 2008. 30th Annual International Conference of the IEEE*, pp. 2489 –2492, aug. 2008.

[14] W. Chan and H. L. Galiana, "Integrator function in the oculomotor system is dependent on sensory context," *Journal of Neurophysiology*, vol. 93, no. 6, pp. 3709–3717, 2005.

[15] B. J. Winterson and H. Collewun, "Microsaccades during finely guided visuomotor tasks," *Vision Research*, vol. 16, no. 12, pp. 1387 – 1390, 1976.